

Modeling Short Over-Dispersed Spike-Train Data: A Hierarchical Parametric Empirical Bayes Framework

Qi She, Beth Jelfs, Rosa H.M.Chan

December 3, 2024

Abstract

In this letter, a Hierarchical Parametric Empirical Bayes (**HPEB**) model is proposed to fit spike count data. We have integrated Generalized Linear Models and empirical Bayes theory to simultaneously solve three problems: (1) over-dispersion of spike count values; (2) biased estimation of the maximum likelihood method and (3) difficulty in sampling from high-dimensional data with fully Bayes estimators. We apply the model to study both simulated data and experimental neural data from the retina. The simulation results indicate that the new model can estimate both the weights of connections among neural populations and the output firing rates efficiently and accurately. The results from the retinal datasets show that the proposed model outperforms both standard Poisson and Negative Binomial Generalized Linear Models in terms of the prediction log-likelihood of held-out datasets.

1 Introduction

Functions of neural networks depend on connectivity at different levels of the network. Hence, if we want to investigate properties of the network it is important to be able to reconstruct the connectivity. Currently, this relationship is constructed by reverse-engineering the connectome, using invasive neural recording techniques, to build a mechanistic model. However, this approach

is time-consuming [1, 2] and as such, a viable alternative is to take an input-output driven approach and analyze the connectivity from neural activities [3]. In particular, functional connectivity is a type of neural circuitry, which is inferred from statistical dependences within the neural data [4]. Accurate reconstruction of these functional dependence patterns would allow the use of graph theory to further analyze the network properties. Crucial to such an approach is how to model the relationship between the spike count data in order to build a reasonable estimate of these dependences.

With the increasing accessibility of datasets containing simultaneously recorded spike-train data, it is now possible to reconsider the efficiencies of different methods for extracting functional dependences at a neuronal level. Various approaches to modeling the statistical dependences of multiple spike trains exist, all of which require certain assumptions about the relationships within the data. Two commonly used methods are Generalized Linear Models (GLMs) and latent variable models. The advantage of GLMs is that they can take into account stimuli, self-spiking history, and outputs of trigger neurons [5, 6, 7, 8]. Whereas latent variable models are used to visualize the modeling structure through graphical representation and relate latent variables to the manifest variables [9, 10, 11, 12]. Both of these methods assume that the spike count data are Poisson distributed. While the Poisson assumption works well in most cases [13], the Poisson model is established on the assumption that the expected mean value of the spike count is equal to the variance. This ignores the fact that in some cases the variance of the spike count could be much larger than its mean [14], that is, the data is over-dispersed. The *Negative Binomial* (NB) model has been proposed to handle over-dispersion cases when dealing with modeling count data [15]. Yet, despite the advantages of the NB model, when the spike train data is sparse and a large number of neurons are recorded simultaneously, the accuracy of the estimated coefficients using GLMs with NB response is low [16]. While group *LASSO* can be applied to address the overfitting problem the computational cost of such an approach is high.

At the same time, the estimation of GLMs is biased if the length of data is limited, be that either due to the length of the experiment or the need for real-time inference [17, 18, 19]. This is because traditional GLMs do not have reasonable shrinkage which in turn makes the estimation biased. When the model selected does not match the simulated data, further modification needs to be made to the model. If we have subjective information about our parameters, using a Bayesian

model can provide advantageous prior information. The two major classes of Bayes inference are fully Bayes inference and empirical Bayes inference. The former gives a hyperprior based on hyperparameters, while the latter obtains the information of unknown parameters from the joint marginal distribution of the training data. Fully Bayes has good shrinkage but has difficulties when sampling from high-dimensional data [20]. Instead, empirical Bayes offers a shrinkage estimator with much lower computational cost. Hence, by combining empirical Bayes with NB GLMs we can produce an estimator which should be capable of handling both over-dispersion and short data lengths.

For empirical Bayes estimation, marginal maximum likelihood estimation of hyperparameters is required, but normally, in hierarchical modeling, it is hard to obtain closed-forms of the estimators of the hyperparameters. Thus, numerical optimization is applied to search for optimal hyperparameters. When determining the search direction of the optimal hyperparameters, Newton’s method is used to find better approximations of the unknown variables. However, in each iteration, Newton’s method has a large computational cost when computing the Jacobian or Hessian matrix, and sometimes the Jacobian or Hessian matrix are unavailable. To circumvent these problems, a Quasi-Newton method to approximate the Hessian matrix can be used. The *Davidon-Fletcher-Powell (DFP)* [21] formula was proposed to approximate the Hessian matrix but is not numerically stable in high-dimensional hyperparameter searches. Thus, *Broyden-Fletcher-Goldfarb-Shanno (BFGS)* [22] was proposed to obtain the search direction using matrix multiplication instead of solving a linear system of equations. It is more numerically stable, and has very effective “self-correcting properties” superior to *DFP* [23], hence, performing better in practice.

In this letter, we propose a hierarchical framework for parametric empirical Bayes (**HPEB**) inference on multiple spike trains. The hierarchical framework is structured such that the spike count data is modeled using a NB GLMs which is then used to infer the parameters of the prior distribution of the empirical Bayes. The purpose of this approach is to solve three problems:

1. Over-dispersion when the spike count variance is greater than its mean value;
2. Bias in estimation using traditional GLMs when the data length is short;
3. Inefficient estimation and inference for both simulated and experimental datasets.

This letter is organised as follows. In Section 2 we introduce the **HPEB**. Section 3 discusses esti-

mation of the latent variables of the **HPEB**, via numerical optimization of the marginal maximum likelihood, and the roles of these variables. Results for both simulated and experimental data are presented in Section 4. Discussion of the main contributions and findings of this letter are given in Section 5. Finally Section 6 concludes the letter.

2 Modeling

In this section, we introduce the **HPEB** model and derive the **HPEB** estimator. We then analyze the performance of this estimator, and give an explanation of the advantage of the empirical Bayes estimator. The left panel of Fig. 1 illustrates the network in the simplest case considered in this letter, the connections among the neural populations are denoted as “functional dependences”. Based on this representation the **HPEB** model aims to predict the underlying firing rates and estimate the observed spike count data. Information which can later be used to estimate the functional connectivity properties of the network. The right panel of Fig. 1 shows the structure of our model and the latent variables of these “functional dependences”. The data length (the number of time bins) is equal to K and μ_i is the formation of the GLMs by input regressors x_i , weights vector ω , and the link function determined by γ . The actual mean firing rate θ_i is controlled by σ (the degree of freedom of the prior distribution), which together with the key parameter for the NB distribution r , generate the observed spike count data Y_i .

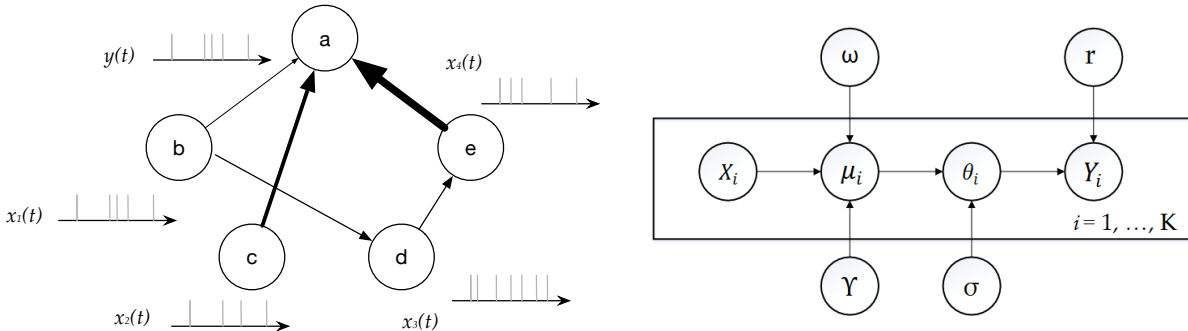


Figure 1: Network Model and Graphical representation. *left panel*: Neuron #a is the target neuron, Neuron #b, #c, #d and #e are trigger neurons used as input regressors. The model aims to predict the underlying firing rate of #a, and derive the spike count estimator. The observed data are multiple spike trains recorded simultaneously; *right panel*: Graphical visualization of the proposed model.

2.1 Negative Binomial Generalized Linear Model

If we consider the case of over-dispersion of the spike count data, the neuronal response can be modelled as a NB distribution. The NB distribution has the assumption that the variance of the spike count data is larger than its mean value and at the same time can also be represented as a Gamma-Poisson mixture. The Gamma-Poisson mixture, models the spike count of the j -th trial at time i , denoted as y_{ij} , as a Poisson distribution, while the mean value λ_i , of the count data from time bin i , becomes a Gamma distribution. These processes are given as

$$y_{ij} | \lambda_i \sim \text{Pois}(\lambda_i) = \frac{\lambda_i^{y_{ij}}}{y_{ij}!} e^{-\lambda_i}; \quad (1)$$

$$\lambda_i | r, \theta_i \sim \text{Ga} \left(r, \frac{\theta_i}{1 - \theta_i} \right) = \lambda_i^{r-1} \frac{\exp \left(-\lambda_i \frac{\theta_i}{1 - \theta_i} \right)}{\left(\frac{1 - \theta_i}{\theta_i} \right)^r \Gamma(r)}. \quad (2)$$

Thus, by combining these two processes, we can model the spike count response as a NB distribution in the form

$$y_{ij} | r, \theta_i \sim \text{NB}(r, \theta_i) = \binom{r + y_{ij} - 1}{y_{ij}} (\theta_i)^r (1 - \theta_i)^{y_{ij}}, \quad (3)$$

where $(1 - \theta_i)$ represents the firing probability at time i , r is the number of failures (zeros) and j is the trial number. The performance of the NB distribution is shown in the left panel of Fig. 2 illustrating the effect of decreasing values of θ_i on the mean and variance. The super-Poisson variability makes this model appropriate for use with over-dispersed data.

The hierarchical model links the mean firing rate θ_i with the Bayesian prior. We have selected the *Beta* distribution as the prior distribution as it is the conjugate prior of the NB distribution likelihood making derivation of a closed-form posterior distribution possible. The *Beta* distribution of θ_i is given by

$$\theta_i \sim \text{Beta}(\alpha_i, \beta_i) = \frac{\theta_i^{\alpha_i-1} (1 - \theta_i)^{\beta_i-1}}{\text{B}(\alpha_i, \beta_i)}; \quad (4)$$

$$\text{B}(\alpha_i, \beta_i) = \frac{\Gamma(\alpha_i)\Gamma(\beta_i)}{\Gamma(\alpha_i + \beta_i)}. \quad (5)$$

The hyperparameters of the distribution are α_i and β_i , $\text{B}(\alpha_i, \beta_i)$ is the beta function, and it is known that $\text{B}(\alpha_i, \beta_i) = \int_0^1 x^{\alpha_i-1} (1 - x)^{\beta_i-1} dx$, which can also be represented using Gamma function $\Gamma(\cdot)$, which is shown in Eq. (5), here $\Gamma(t) = \int_0^\infty x^{t-1} e^{-x} dx$, . We define the open parameter

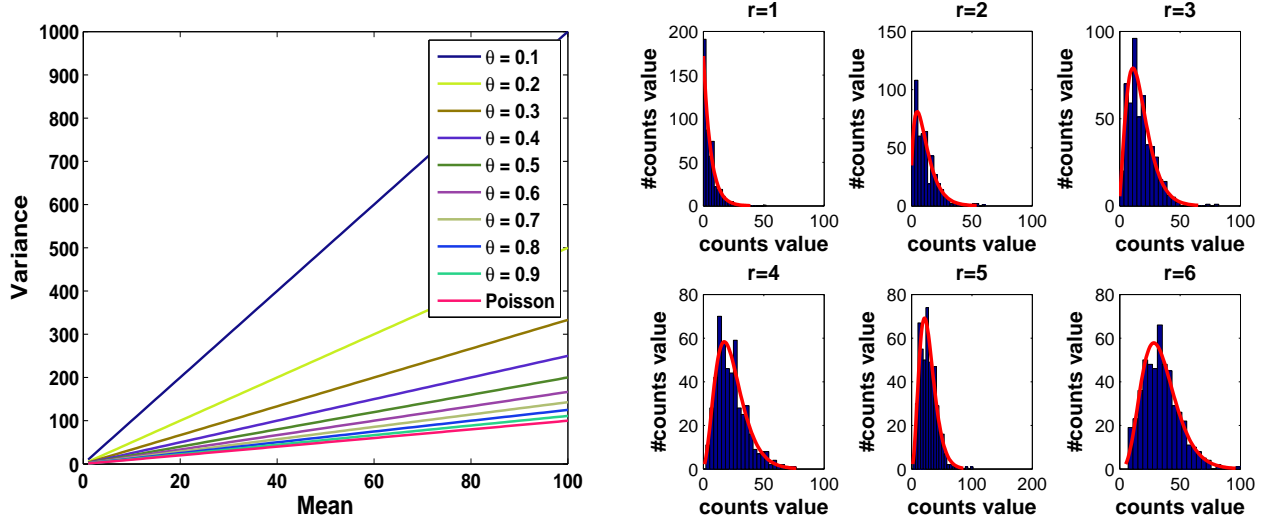


Figure 2: *left panel*: Relationship between mean and variance for different settings of θ , which shows the super-Poisson variability of the NB model compared with the Poisson model. The smaller θ is, more significant the super-Poisson effect is; *right panel*: NB distribution with different r .

$\sigma = \alpha_i + \beta_i$, which can be viewed as the degree of freedom of the prior distribution. The prior mean, $\mathbb{E}(\theta_i | \alpha_i, \beta_i) = \mu_i$, is given by $\mu_i = \frac{\alpha_i}{\alpha_i + \beta_i}$, because we assume $\sigma = \alpha_i + \beta_i$, then we can rearrange to get $\alpha_i = \sigma \mu_i$ and $\beta_i = \sigma(1 - \mu_i)$.

To link the prior distribution with GLMs, the prior mean, μ_i , is modelled as the predictor for a GLM. In this case, it is necessary and reasonable to scale the underlying firing rate between 0 and 1, which can be achieved using a family of link functions. Thus, the prior mean becomes

$$\mu_i = g^{-1}(\mathbf{x}_i^T \boldsymbol{\omega}) = 1 - \left(\gamma e^{\mathbf{x}_i^T \boldsymbol{\omega}} + 1 \right)^{-\frac{1}{\gamma}}, \quad (6)$$

where \mathbf{x}_i is a given vector of neurons' input as regressors, typically spike counts from other neurons or spiking history of neuron activities, $\boldsymbol{\omega}$ is a vector of weights capturing the directed effect of the neural population on the target neuron, and γ is a flexible parameter determining the specific form of link function $g(\cdot)$. The latent variable γ for the link function is generated from the data itself, which ensures the flexibility of the nonlinear transformation of the regressors. We select this link family because it can represent many widely used link functions, for instance, the logit function when $\gamma = 1$. It also constrains the prior mean, modeled as the mean value of the firing rate, to $\mu_i > 0$.

2.2 HPEB Estimator

Because the *Beta* distribution is the conjugate prior for the NB likelihood function, we can derive the closed form of the posterior distribution in the form of the *Beta Negative Binomial* distribution

$$\theta_i | y_{ij} \sim \text{Beta} \left(\alpha_i + n_i r, \beta_i + \sum_{j=1}^{n_i} y_{ij} \right) = \text{Beta} \left(\sigma \mu_i + n_i r, \sigma (1 - \mu_i) + n_i \bar{y}_i \right), \quad (7)$$

where n_i is the number of trials of the i -th time bin and \bar{y}_i is the mean value of the count data across all trials at each bin i . Substituting the inverse link function of μ_i into Eq. (7) we get

$$\theta_i | y_{ij} \sim \text{Beta} \left(\sigma g^{-1}(\mathbf{x}_i^T \boldsymbol{\omega}) + n_i r, \sigma \left(1 - g^{-1}(\mathbf{x}_i^T \boldsymbol{\omega}) \right) + n_i \bar{y}_i \right). \quad (8)$$

Our proposed **HPEB** estimator is defined as the expected value of the posterior distribution of θ_i , the **HPEB** estimator is given as

$$\theta_i^{HPEB} = \mathbb{E}(\theta_i | y_{ij}, r, \boldsymbol{\omega}, \sigma, \gamma) = \frac{n_i r + \sigma g^{-1}(\mathbf{x}_i^T \boldsymbol{\omega}, \gamma)}{n_i r + n_i \bar{y}_i + \sigma}. \quad (9)$$

The estimator has a group of unknown parameters $\{r, \boldsymbol{\omega}, \sigma, \gamma\}$ to estimate, the functions and effects of which will be discussed in Section 3.2. Having obtained the final estimator, its structure can then be used to determine the advantages of this estimator. Actually, the estimator can be viewed as a combination of the prior mean GLMs and the observed data. In order to have a clear representation of our proposed estimator, we rewrite Eq. (9) as a convex combination of two components (the GLMs and the Observations)

$$\begin{aligned} \theta_i^{HPEB} &= \frac{n_i r + \sigma g^{-1}(\mathbf{x}_i^T \boldsymbol{\omega}, \gamma)}{n_i r + n_i \bar{y}_i + \sigma} \\ &= \frac{n_i r + n_i \bar{y}_i}{n_i r + n_i \bar{y}_i + \sigma} \times \frac{n_i r}{n_i r + n_i \bar{y}_i} + \frac{\sigma}{n_i r + n_i \bar{y}_i + \sigma} \times g^{-1}(\mathbf{x}_i^T \boldsymbol{\omega}, \gamma). \end{aligned} \quad (10)$$

We assign the weight of the observation component as $\pi_i = \frac{n_i r + n_i \bar{y}_i}{n_i r + n_i \bar{y}_i + \sigma}$, and then $1 - \pi_i = \frac{\sigma}{n_i r + n_i \bar{y}_i + \sigma}$.

Thus, Eq. (10) is simplified as

$$\theta_i^{HPEB} = \pi_i \times \frac{n_i r}{n_i r + n_i \bar{y}_i} + (1 - \pi_i) \times g^{-1}(\mathbf{x}_i^T \boldsymbol{\omega}, \gamma). \quad (11)$$

Hence, the weights assigned to the observations, $\frac{n_i r}{n_i r + n_i \bar{y}_i}$, and to the prior mean value, $g^{-1}(\mathbf{x}_i^T \boldsymbol{\omega}, \gamma)$ are controlled by the value π_i , where π_i is a shrinking coefficient, and $0 \leq \pi_i \leq 1$. When $\pi_i = 1$, it

results in no shrinkage of θ_i^{HPEB} from the observations to the prior mean value. Thus, θ_i^{HPEB} is a shrinkage estimator. The final estimated values of the degree of freedom of the prior distribution σ , and the number of failures r , determine the value of π_i . That is to say, when $\sigma \gg n_i r + n_i \bar{y}_i$, the estimator is approaching the prior mean, while when $\sigma \ll n_i r + n_i \bar{y}_i$, the estimator is determined by the observations. This structure has the advantage that all the latent variables (determining the weights) are learned from the data itself and the final estimator can be obtained by adjusting the weights of the prior information and the observations. Furthermore, the measurement of the variance of posterior distribution is

$$\text{Var}(\theta_i | y_{ij}, r, \omega, \sigma, \gamma) = \frac{\left(\frac{n_i r + \sigma g^{-1}(\mathbf{x}_i^T \omega, \gamma)}{n_i r + n_i \bar{y}_i + \sigma} \right)^2 - \left(\frac{n_i r + \sigma g^{-1}(\mathbf{x}_i^T \omega, \gamma)}{n_i r + n_i \bar{y}_i + \sigma} \right)}{n_i r + n_i \bar{y}_i + \sigma + 1}. \quad (12)$$

Assuming the estimations of r and σ are accurate, $n_i r + n_i \bar{y}_i + \sigma$ are fixed, and the variance of the posterior of the mean firing rate θ_i is a quadratic function of the prior mean value GLMs. The variance can achieve the global maximum when $g^{-1}(\mathbf{x}_i^T \omega, \gamma) = \frac{1}{2} n_i \bar{y}_i - \frac{1}{2} n_i r + \frac{1}{2}$, and

$$\text{Var}_{\max}(\theta_i | y_{ij}, r, \omega, \sigma, \gamma) = \frac{1}{4 \times (n_i r + n_i \bar{y}_i + \sigma + 1)}. \quad (13)$$

3 Marginal Maximum Likelihood to Estimate Latent Variables

In this section, we discuss the estimation of latent variables using marginal maximum log likelihood, and give the derivation of gradient functions for each variables. Finally, we talk about the roles of each latent variables of our model and how to adjust the initial value before optimization based on prior knowledge to get more stable and accurate optimal results.

After deriving the **HPEB** estimator from Section 2.2, we need to estimate the parameters $r, \omega, \gamma, \sigma$. The unknown parameters can be estimated utilizing the marginal distribution. The Marginal maximum likelihood approach does not include any assumptions on the hyperparameters, it can have lower computational cost. By integrating y_{ij} we can obtain the marginal log

likelihood (MLL) of the conditional posterior distribution as

$$\begin{aligned}
\ell(r, \boldsymbol{\omega}, \sigma, \gamma) \propto & \sum_{i=1}^K \sum_{j=1}^{n_i} \left[\log \Gamma\left(r + \sigma g^{-1}(\mathbf{x}_i^T \boldsymbol{\omega}, \gamma)\right) \right. \\
& + \log \Gamma\left(y_{ij} + \sigma - \sigma g^{-1}(\mathbf{x}_i^T \boldsymbol{\omega}, \gamma)\right) + \log \Gamma(r + y_{ij}) \\
& + \log \Gamma(\sigma) - \log \Gamma(r + y_{ij} + \sigma) - \log \Gamma(r) \\
& \left. - \log \Gamma\left(\sigma g^{-1}(\mathbf{x}_i^T \boldsymbol{\omega}, \gamma)\right) - \log \Gamma\left(\sigma - \sigma g^{-1}(\mathbf{x}_i^T \boldsymbol{\omega}, \gamma)\right) \right], \tag{14}
\end{aligned}$$

where K is the data length (the number of time bins). We estimate the parameters $r, \boldsymbol{\omega}, \sigma, \gamma$, by maximizing the MLL and then substitute them into the **HPEB** estimator.

3.1 Quasi-Newton Numerical Optimization

MLL estimation of the hyperparameters $\hat{r}, \hat{\boldsymbol{\omega}}, \hat{\sigma}, \hat{\gamma}$ is conducted by maximizing the log likelihood function. In this case, closed-forms are not available, thus, numerical optimization is required. Here, we apply the Quasi-Newton optimization method to approximate the Hessian matrix. At each iteration we need to approximate the Hessian matrix, in order to give more stable and accurate convergence we need to provide the gradient function of each element. We derive the gradient functions of $\hat{r}, \hat{\boldsymbol{\omega}}, \hat{\sigma}, \hat{\gamma}$ respectively, as,

$$\begin{aligned}
\frac{\partial \ell(r, \boldsymbol{\omega}, \sigma, \gamma)}{\partial r} &= \sum_{i=1}^K \sum_{j=1}^{n_i} \Psi\left[r + \sigma g^{-1}(\mathbf{x}_i^T \boldsymbol{\omega}, \gamma)\right] + \Psi(r + y_{ij}) - \Psi(r + y_{ij} + \sigma) - \Psi(r); \\
\frac{\partial \ell(r, \boldsymbol{\omega}, \sigma, \gamma)}{\partial \omega_p} &= \sigma \sum_{i=1}^K \sum_{j=1}^{n_i} \frac{\partial g^{-1}(\mathbf{x}_i^T \boldsymbol{\omega}, \gamma)}{\partial \omega_p} (A_i - B_{ij}); \\
\frac{\partial \ell(r, \boldsymbol{\omega}, \sigma, \gamma)}{\partial \sigma} &= \sum_{i=1}^K \sum_{j=1}^{n_i} \left\{ A_i g^{-1}(\mathbf{x}_i^T \boldsymbol{\omega}, \gamma) + B_{ij} \left[1 - g^{-1}(\mathbf{x}_i^T \boldsymbol{\omega}, \gamma) \right] + C_{ij} \right\}; \\
\frac{\partial \ell(r, \boldsymbol{\omega}, \sigma, \gamma)}{\partial \gamma} &= \sum_{i=1}^K \sum_{j=1}^{n_i} \frac{\partial g^{-1}(\mathbf{x}_i^T \boldsymbol{\omega}, \gamma)}{\partial \gamma} (A_i - B_{ij}). \tag{15}
\end{aligned}$$

For clarity, we have defined A_i, B_{ij}, C_{ij} :

$$\begin{aligned}
A_i &= \Psi\left(r + \sigma g^{-1}(\mathbf{x}_i^T \boldsymbol{\omega}, \gamma)\right) - \Psi\left(\sigma g^{-1}(\mathbf{x}_i^T \boldsymbol{\omega}, \gamma)\right); \\
B_{ij} &= \Psi\left(y_{ij} + \sigma - \sigma g^{-1}(\mathbf{x}_i^T \boldsymbol{\omega}, \gamma)\right) - \Psi\left(\sigma - \sigma g^{-1}(\mathbf{x}_i^T \boldsymbol{\omega}, \gamma)\right); \\
C_{ij} &= \Psi(\sigma) - \Psi(r + y_{ij} + \sigma), \tag{16}
\end{aligned}$$

where $\Psi(\cdot)$ is the digamma function, such that $\Psi(x) = \frac{\partial \log \Gamma(x)}{\partial x}$, ω_p is the individual element in the vector space ω with $p = (1, 2, \dots, N)$ and N is the number of neurons involved in the functional network. The gradients of $g^{-1}(\mathbf{x}_i^T \omega, \gamma)$ for ω_p and γ are given as

$$\begin{aligned} \frac{\partial g^{-1}(\mathbf{x}_i^T \omega, \gamma)}{\partial \omega_p} &= x_p e^{x_i^T \omega} \left(\gamma e^{x_i^T \omega} + 1 \right)^{-\frac{1}{\gamma}-1}; \\ \frac{\partial g^{-1}(\mathbf{x}_i^T \omega, \gamma)}{\partial \gamma} &= - \left(\gamma e^{x_i^T \omega} + 1 \right)^{-\frac{1}{\gamma}} \left[\frac{\log \left(\gamma e^{x_i^T \omega} + 1 \right)}{\gamma^2} - \frac{e^{x_i^T \omega}}{\gamma \left(\gamma e^{x_i^T \omega} + 1 \right)} \right]. \end{aligned} \quad (17)$$

We use the *Broyden-Fletcher-Goldfarb-Shanno (BFGS)* [22] algorithm to maximize the MLL. This is an iterative method suitable for solving unconstrained nonlinear optimization problems such as maximizing MLL presented here. Although we provide gradient functions to try to ensure stable and accurate optimization, when randomly selecting initial values it can still sometimes lead to $\gamma < 0$, which does not guarantee a mean firing rate within $(0, 1)$. In this case, we also provide the constraint $\gamma > 0$ using Sequential Quadratic Programming (*SQP*) [24], with the Quasi-Newton method also applied at each updating step. Our first step is to form a quadratic program and find a line search direction by minimizing the quadratic subproblem. We set $\zeta = (r, \omega_{1 \times N}, \sigma, \gamma)$, and form a Lagrangian function as

$$L(\zeta, \mathbf{k}) = \ell(\zeta) + \sum_{m=1}^{N+3} k_m \zeta_m, \quad (18)$$

where, $\mathbf{k} = \{k_1, k_2, \dots, k_{N+3}\}$ is the Lagrangian coefficient, the total number of latent variables is $N + 3$, N (the number of neurons involved in the functional network) is equivalent to the length of vector ω and (r, σ, γ) are the other three parameters. We then form the quadratic programming subproblem

$$\min_{\mathbf{d} \in \mathbb{R}^d} \nabla \ell^T(\zeta) \mathbf{d} + \frac{1}{2} \mathbf{d}^T \nabla^2 L(\zeta, \mathbf{k}) \mathbf{d}; \quad (19)$$

$$\nabla \zeta_m^T \mathbf{d} + \zeta_m \leq 0, m = 1, \dots, N + 3. \quad (20)$$

These quadratic problems can be solved using an active-set algorithm [25]. At each iteration step t , we find the linear search direction \mathbf{d} , and then use a line search procedure to find the step length parameter Δ which achieves a sufficient decrease in the merit function. We update the group parameters ζ until converged as below

$$\zeta(t+1) = \zeta(t) + \Delta_t \times \mathbf{d}(t). \quad (21)$$

3.2 The Role of Latent Variables

The latent variables in the **HPEB** estimator play different roles in explaining our dataset. In this section, we discuss each of them and try to find rules to adjust their initial values in order to provide good estimations.

- r determines the NB response. In real situations, the actual firing rate of underlying neural populations may not be very high, such as in the hippocampal formation. In order to get reasonable spike count estimations, we should make sure the initial value of r is small as this helps the spike counts observations match the low firing rates. In other words, if we believe a brain area has a high firing rate, such as in the motor cortex, we can tune r to be larger initially. For simplicity, we have made r the same across all time steps, which means for the whole data length $i = 1, 2, \dots, K$, $r_i = r$. In the right panel of Fig. 2, we keep the same underlying firing rate and show the influence of different r on the spike count data.
- ω is a vector of weights capturing the directed effect of existing neurons on the target neuron. The vector can also include other factors such as the spiking history of target neurons, external stimuli e.g. if we have prior knowledge, for instance the pixels of an image shown to excite the retinal neurons. These weights can be positive or negative, which can be explained as neurons having either an excitatory or inhibitory effect on the target neuron. We test, with our simulated data, the ability to capture the excitatory and inhibitory effect of functional circuitry. Without loss of generality, the initial value of each element in ω is randomly chosen from $(-1, 1)$.
- σ is the degree of freedom of the *beta* distribution. From Eq. (10), we can see our proposed estimator is the weighted combination of the observed data ($\theta_i^{ob} = \frac{n_i r}{n_i r + n_i \bar{y}_i}$) and traditional GLM estimation ($\theta_i^{GLM} = g^{-1}(\mathbf{x}_i^T \boldsymbol{\omega}, \gamma)$). The weights of each component are $\pi_i = \frac{n_i r + n_i \bar{y}_i}{n_i r + n_i \bar{y}_i + \sigma}$ and $1 - \pi_i = \frac{\sigma}{n_i r + n_i \bar{y}_i + \sigma}$. Thus, if σ is large enough, the proposed method is close to prior mean GLMs; when it is smaller, the estimator is approaching the observed data. The initial value of σ is determined by the number of trials n_i , such that, $\sigma \propto n_i$. This means the more trials we have, the more information we can have about the expectation of the mean spike counts.

- γ selects the best fit of link function for our dataset. When $\gamma = 1$, it is commonly used logit function, when γ is approaching 0, it becomes the complementary log-log link. Commonly, GLMs choose the link function by specifying a parametric link. Our work determines the unknown parameter by MLL, learning from the dataset itself to automatically select a suitable link function. The initial value of γ is determined to result in relatively low firing rate, which has empirically been shown to have good performance for spike count prediction.

3.3 Summary of Hierarchical Empirical Bayes Inference

In this subsection, we summarize our algorithm, the steps required for empirical Bayes inference on hierarchical models are shown in Algorithm 1.

4 Results

In this section, we test our methods on both simulated and experimental data. The simulated data is generated from the process outlined in the previous section, and the experimental datasets include four different experiments with different numbers of neurons from the retina. This data is used for validating the stability and fitness of our model for real spike count data.

4.1 Simulated Data

Our inference method was first tested on data generated from the model shown in Fig. 1. The network sizes are 10, 20 and 50. Using the simulated dataset, we conducted three tests:

- Interaction predictions. We randomly assigned excitatory or inhibitory weights to the neural population. Our goal was to identify whether we could recover the weights of the interactions.
- Performance of the **HPEB** estimator. In the simulation process, we have the background truth about the underlying firing rate. We tested the performance of **HPEB** estimator using mean square error (MSE).

Algorithm 1 Steps for Empirical Bayes inference on hierarchical models

Input: $\mathbf{x}_i = [x_{i1}, x_{i2}, \dots, x_{iN}]$, y_{ij} ($i = 1, \dots, K$ and $j = 1, \dots, n_i$).

Output: $\mathbb{E}(\theta_i | \hat{r}, \hat{\omega}, \hat{\sigma}, \hat{\gamma})$, θ_i is the underlying firing rate of target neuron.

- 1: Initialize $r, \omega, \sigma, \gamma$.
- 2: Form the linear regressors $\eta_i = \mathbf{x}_i^T \omega$.
- 3: Form the extended link function $\eta_i = g(u_i, \gamma)$.
- 4: Prior information is derived as $u_i = g^{-1}(\mathbf{x}_i^T \omega, \gamma)$.
- 5: Construct *beta negative binomial* marginal distribution log-likelihood function

$$\begin{aligned} \ell(r, \omega, \sigma, \gamma) \propto & \sum_{i=1}^K \sum_{j=1}^{n_i} \left[\log \Gamma(r + \sigma g^{-1}(\mathbf{x}_i^T \omega, \gamma)) \right. \\ & + \log \Gamma(y_{ij} + \sigma - \sigma g^{-1}(\mathbf{x}_i^T \omega, \gamma)) + \log \Gamma(r + y_{ij}) \\ & + \log \Gamma(\sigma) - \log \Gamma(r + y_{ij} + \sigma) - \log \Gamma(r) \\ & \left. - \log \Gamma(\sigma g^{-1}(\mathbf{x}_i^T \omega, \gamma)) - \log \Gamma(\sigma - \sigma g^{-1}(\mathbf{x}_i^T \omega, \gamma)) \right]. \end{aligned}$$

- 6: Derive the gradient function of each latent variable

$$\nabla \ell(r, \omega, \sigma, \gamma) = \left(\frac{\partial \ell}{\partial r}, \frac{\partial \ell}{\partial \omega_p}, \frac{\partial \ell}{\partial \sigma}, \frac{\partial \ell}{\partial \gamma} \right).$$

- 7: Apply *BFGS* to determine linear search direction \mathbf{d} .
- 8: Find the marginal maximization log-likelihood estimations of $\hat{r}, \hat{\omega}, \hat{\sigma}, \hat{\gamma}$, calculating the empirical Bayes estimation of $\mathbb{E}(\theta_i | \hat{r}, \hat{\omega}, \hat{\sigma}, \hat{\gamma})$ as

$$\theta_i^{HPEB} = \mathbb{E}(\theta_i | \hat{r}, \hat{\omega}, \hat{\sigma}, \hat{\gamma}) = \frac{n_i \hat{r} + \hat{\sigma} g^{-1}(\mathbf{x}_i^T \hat{\omega}, \hat{\gamma})}{n_i \hat{r} + n_i \bar{y}_i + \hat{\sigma}}.$$

- Comparison with traditional modeling methods. The Poisson and NB GLMs can also capture the excitatory and inhibitory relationships, hence, we compared them with our proposed estimator by predicting spike count data on held-out datasets after training each model.

A range of configurations of the parameters are shown in the Table 1. N_s is the number of trials of each spike train, N is the number of neurons in our simulation, and K represents the data length (bins) of each time series in the test set. The combination of these parameters provides different types of observed spike count data. Table 2 shows a comparison of the MSE for our simulated dataset of the standard Poisson GLM and the NB GLM with the **HPEB** model. In order to benchmark the three methods, we created 10 random train and test splits from different data lengths K , and performed 10-fold cross-validation with 8 splits used for training and 2 splits used for testing. Each model is trained using the training set and then tested by computing the MSE between the estimated spike count data and the true value for 50 randomly selected initializations of the unknown parameters. Comparing the 4 configurations in Table 2 and the left panel of Fig. 3, we can find (1) increasing N_s and K gives better prediction; and (2) having more trials (larger N_s) outperforms having longer data length (larger K). The scatter plot in the right panel in Fig. 3 provides us with a clear view of the comparison between true and fitted spike count.

Next, to test the estimation of the actual weights across the neural population we explored *BFGS* method, applied to maximize the marginal likelihood derived for different data lengths. The results shown in Fig. 4 are taken for several combinations of the parameter configurations in Table 1, as we can see: (1) the relative standard error is large when the actual weights are close to 0; and (2) 1000 bins is sufficient to provide accurate and efficient weight estimation.

Table 1: Configurations of the parameters used for the simulated data

N_s	N	K	ω	r	σ	γ
1, 10, 20, 50, 100	10,20,50	100,500,1000,2000	(-1, +1)	1,3,5	50,100,200	1,3,5,7

4.2 Experimental Data

The retinal ganglion cell datasets, curated from CRCNS.org ret-1 [26], contain multi-unit recordings of neurons. We tested 4 datasets containing 37, 26, 15, 14 neurons, respectively. We binned

Table 2: Comparison of the Poisson GLM, NB GLM and HPEB model for $N = 20$, $r = 5$, $\sigma = 50$, $\gamma = 7$

$N_s = 10, K = 500$	MSE	$N_s = 50, K = 500$	MSE	$N_s = 100, K = 500$	MSE
Poisson GLM	0.497	Poisson GLM	0.292	Poisson GLM	0.058
NB GLM	0.497	NB GLM	0.292	NB GLM	0.050
HPEB Model	0.304	HPEB Model	0.264	HPEB Model	0.048
$N_s = 10, K = 1000$	MSE	$N_s = 50, K = 1000$	MSE	$N_s = 100, K = 1000$	MSE
Poisson GLM	0.452	Poisson GLM	0.215	Poisson GLM	0.059
NB GLM	0.450	NB GLM	0.215	NB GLM	0.049
HPEB Model	0.255	HPEB Model	0.175	HPEB Model	0.037
$N_s = 10, K = 2000$	MSE	$N_s = 50, K = 2000$	MSE	$N_s = 100, K = 2000$	MSE
Poisson GLM	0.402	Poisson GLM	0.175	Poisson GLM	0.045
NB GLM	0.380	NB GLM	0.160	NB GLM	0.045
HPEB Model	0.220	HPEB Model	0.160	HPEB Model	0.031

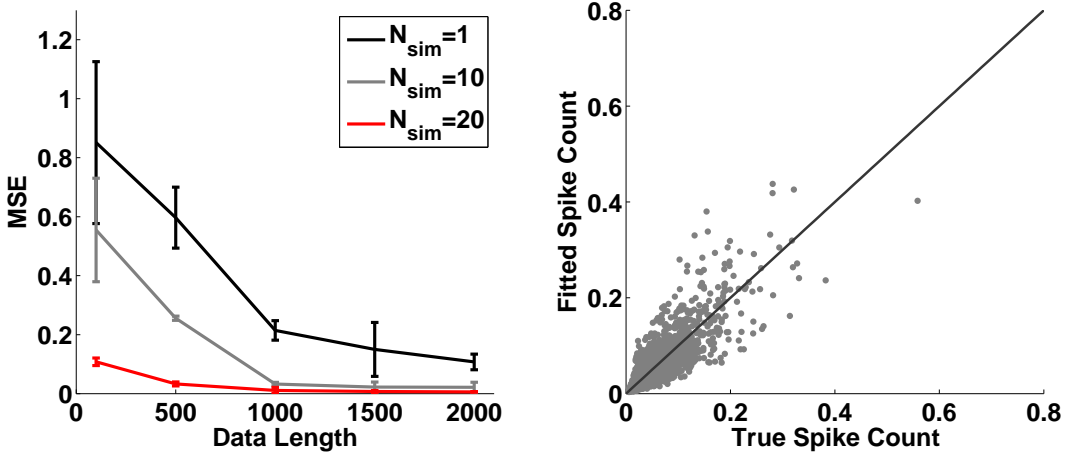


Figure 3: Goodness-of-fit for simulated data - *left panel*: the mean square error across data lengths for different numbers of samples at each time step; *right panel*: scatter plot of fitted spike count and true spike count value with data length 2000.

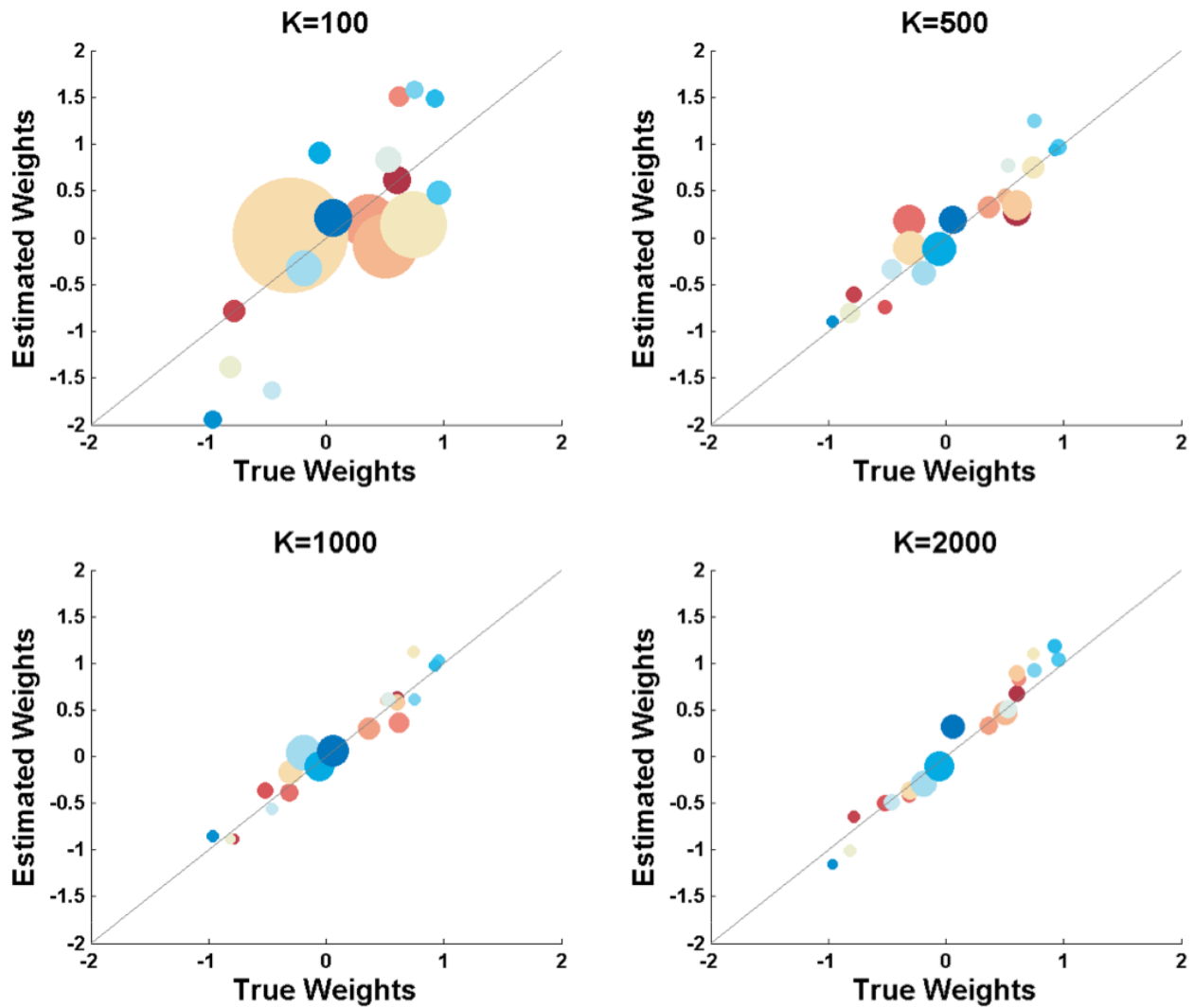


Figure 4: Scatter plots of estimated weights of 20 neurons ($K = 100, 500, 1000, 2000$). Different colors indicate different neurons. The size of the ball shows the relative standard error (standard error/mean value). The initial values of the weights to be optimized was selected randomly from -1 to 1 and simulated 20 times.

the spike counts in 16.7 ms bins, and regressed with other recorded neurons' spike counts, to find the functional dependences among the neural populations. We made 50 random training and testing splits with total data length of 2000 bins, 40 splits are used for training and 10 splits data are used for testing and 50-fold cross validation was used. We used the **HPEB** model to compute held-out datasets log-likelihoods on the test set versus a standard Poisson GLM and NB GLM.

Figures 5 and 6 show the increase in held-out dataset log-likelihood of the **HPEB** model over the Poisson GLM and NB GLM for each of the datasets. Almost all results present higher prediction log likelihood of testing datasets using the **HPEB** model. The improvement compared with the Poisson GLM is much larger than for the NB GLM, indicating the datasets we analyzed have underlying over-dispersed structures. By comparing with the NB GLM, the **HPEB** outperformed it for nearly all recorded neurons, despite the NB GLM having the same assumption as our **HPEB** model for spike count observations. In particular the **HPEB** method outperforms the NB GLM when the data length is short.

5 Discussion

The machine learning community shows great interest in multivariate regression methods, which provide a clear view of the nature relationships using linear and nonlinear effects. [27] have developed fully Bayes inference for NB response, yielding a shrinkage for all latent variables. However, high-dimensional sampling often proves a challenge. [6] gave us a MLE to estimate the unknown parameters, but when the data length is small, the estimation is biased. The **HPEB** estimator developed by us, for finding the latent interactions between neural populations, combines the two above methods. It has the advantage of providing a shrinkage estimator while not needing the intensive computation of the fully Bayes inference for NB response.

In the work presented in this letter, we take advantage of both GLMs and empirical Bayes inference to propose the **HPEB** estimator. We used the negative binomial distribution to model the spike count process of each neuron because it allows for over-dispersion using a dispersion parameter superior to the normal Poisson model. The prior information employed is the beta prior to allow for better posterior distribution derivation. A flexible link function is utilized to model the prior mean with regressors. We use other neurons as the covariates, and infer the functional weights

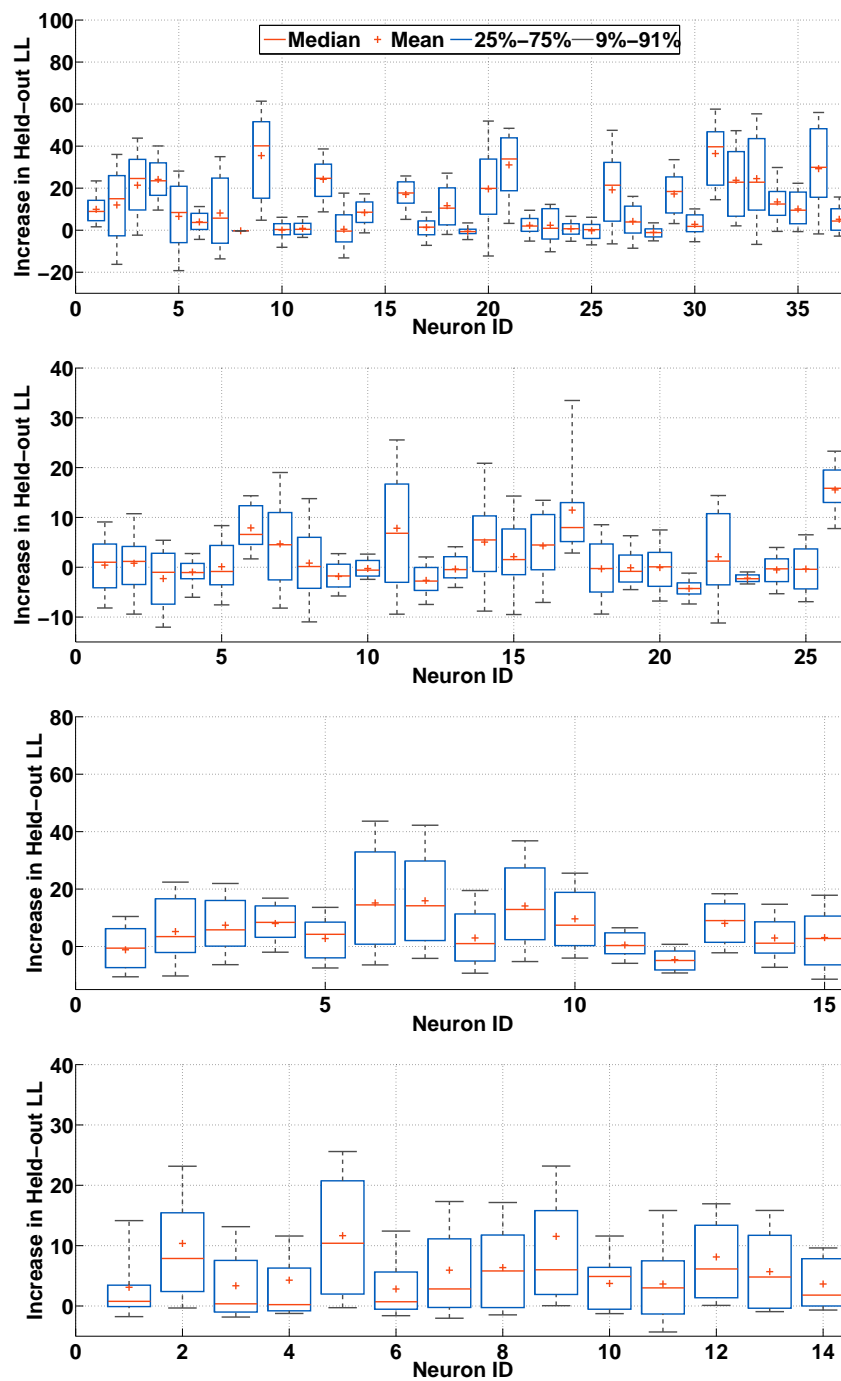


Figure 5: **HPEB** compared with NB GLM: boxplots of the increase in the held-out log likelihood of all neurons in dataset #62413(37 neurons); #62423(26 neurons); #62814(15 neurons); #62871(14 neurons) (from row #1 to row #4).

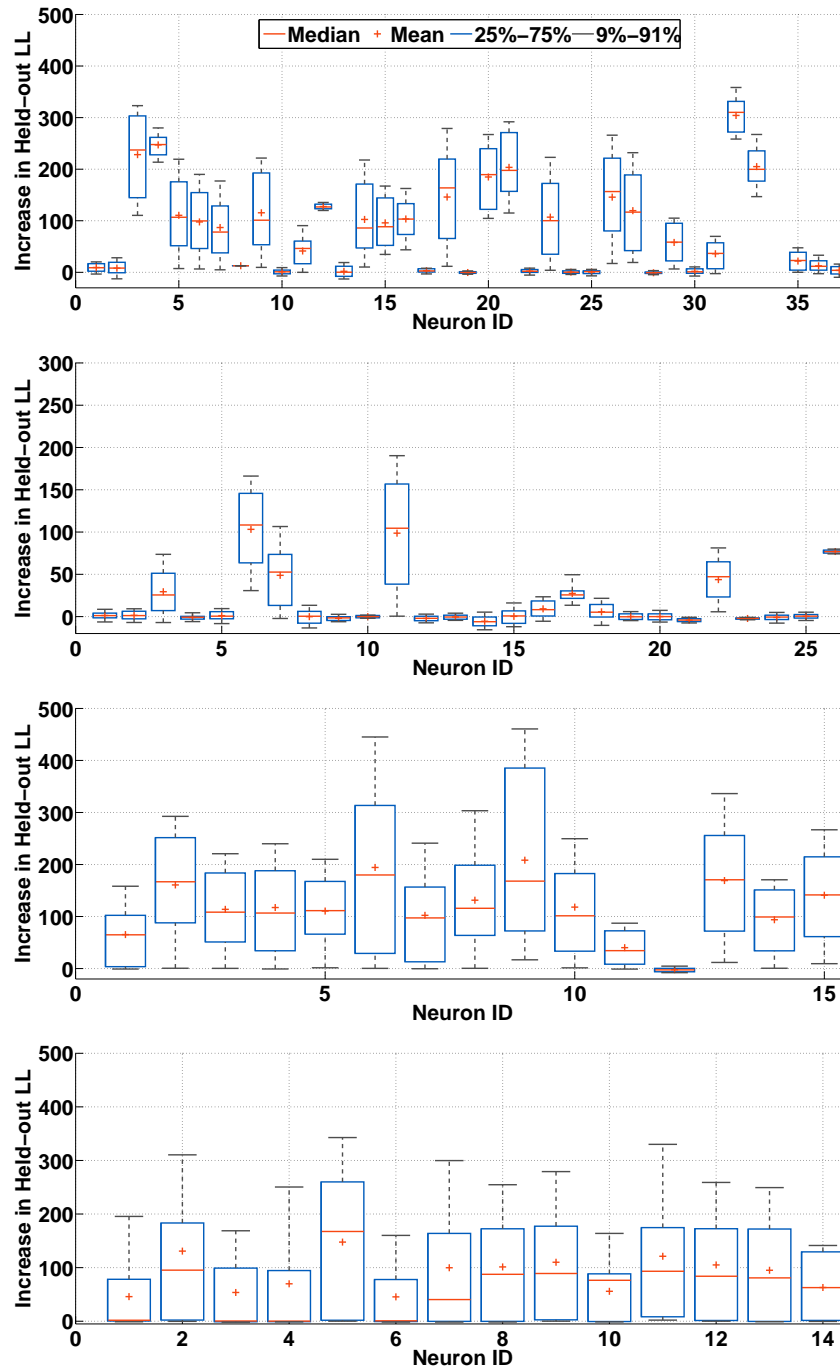


Figure 6: **HPEB** compared with Poisson GLM: boxplots of the increase in the held-out log likelihood of all neurons in dataset #62413(37 neurons); #62423(26 neurons); #62814(15 neurons); #62871(14 neurons) (from row #1 to row #4).

among the neural population. Unlike fully Bayes which utilizes hyperpriors, we instead estimate the hyperparameters by maximizing the marginal likelihood. The proposed **HPEB** estimator is a shrinkage estimator and the weights we estimate can be viewed as the hidden functional structure. We take the neurons as nodes in our functional network, and the observations are the multiple spike trains. Our developed empirical Bayes inference method can be used to identify the neural interactions, including excitatory and inhibitory behaviors. It is also a valid way to estimate the underlying firing rate of each neuron and the corresponding spike count data.

We validate our methods using both simulated data and experimental data taken from retinal neurons. We compared with traditional GLM estimators (both Poisson and Negative Binomial regressions) using intensive simulations to show that the **HPEB** outperforms GLMs in our simulated system. For the simulation data, we can estimate the latent variables accurately by efficiently maximizing the marginal likelihood. The link function is flexible for each dataset instead of using a fixed link like traditional GLMs. For the experimental data, compared with two of the most widely used regression methods: Poisson and NB regressions, there was substantial improvement in the held-out datasets log likelihood when predicting test neuron spike counts. Going forward we are interested in Hebbian learning rules resulting in time-varying weights, which could be used to extend our model. Applying prior knowledge regarding network structure like random, small world or scale-free network could also be a promising avenue for future research.

6 Conclusion

Recently, NB models have been used in systems neuroscience due to their suitability for over-dispersed data [20], but using Bayesian methods is always difficult in conjunction with hierarchical NB modeling. We have made three contributions in our work. First, we propose a shrinkage **HPEB** estimator with less bias and have validated it using both simulated and experimental data. Second, our method is better suited to short over-dispersed spike-train data, while using empirical Bayes can also avoid high computational costs associated with the fully Bayes method. Third, the **HPEB** method has the best performance for (1) identifying interactions among neural populations and (2) estimating spike counts, when compared with both standard Poisson regression and NB regression methods. Our approach can be easily extended with more covariates taken into consideration.

Acknowledgments

The work described in this letter was fully supported by a grant from the Research Grants Council of the Hong Kong Special Administrative Region, China [Project No. CityU110813].

References

- [1] S. M. Plaza, L. K. Scheffer, and D. B. Chklovskii, “Toward large-scale connectome reconstructions,” *Current Opinion in Neurobiology*, vol. 25, pp. 201–210, 2014.
- [2] A.-S. Chiang, C.-Y. Lin, C.-C. Chuang, H.-M. Chang, C.-H. Hsieh, Yeh, *et al.*, “Three-dimensional reconstruction of brain-wide wiring networks in drosophila at single-cell resolution,” *Current Biology*, vol. 21, no. 1, pp. 1–11, 2011.
- [3] H.-J. Park and K. Friston, “Structural and functional brain networks: from connections to cognition,” *Science*, vol. 342, no. 6158, p. 1238411, 2013.
- [4] M. Okatan, M. A. Wilson, and E. N. Brown, “Analyzing functional connectivity using a network likelihood model of ensemble neural spiking activity,” *Neural Computation*, vol. 17, no. 9, pp. 1927–1961, 2005.
- [5] J. W. Pillow, L. Paninski, and E. P. Simoncelli, “Maximum likelihood estimation of a stochastic integrate-and-fire neural model,” in *Advances in Neural Information Processing Systems*, pp. 1311–1318, Citeseer, 2003.
- [6] L. Paninski, J. W. Pillow, and E. P. Simoncelli, “Maximum likelihood estimation of a stochastic integrate-and-fire neural encoding model,” *Neural Computation*, vol. 16, no. 12, pp. 2533–2561, 2004.
- [7] W. Truccolo, U. T. Eden, M. R. Fellows, J. P. Donoghue, and E. N. Brown, “A point process framework for relating neural spiking activity to spiking history, neural ensemble, and extrinsic covariate effects,” *Journal of Neurophysiology*, vol. 93, no. 2, pp. 1074–1089, 2005.

- [8] J. W. Pillow, J. Shlens, L. Paninski, A. Sher, A. M. Litke, E. Chichilnisky, and E. P. Simoncelli, “Spatio-temporal correlations and visual signalling in a complete neuronal population,” *Nature*, vol. 454, no. 7207, pp. 995–999, 2008.
- [9] C. M. Bishop, M. Svensén, and C. K. Williams, “GTM: The generative topographic mapping,” *Neural Computation*, vol. 10, no. 1, pp. 215–234, 1998.
- [10] N. D. Lawrence, “Gaussian process latent variable models for visualisation of high dimensional data,” in *Advances in Neural Information Processing Systems*, vol. 16, pp. 329–336, 2004.
- [11] N. Lawrence, “Probabilistic non-linear principal component analysis with gaussian process latent variable models,” *The Journal of Machine Learning Research*, vol. 6, pp. 1783–1816, 2005.
- [12] K. C. Lakshmanan, P. T. Sadtler, E. C. Tyler-Kabara, A. P. Batista, and M. Y. Byron, “Extracting low-dimensional latent structure from time series in the presence of delays,” *Neural Computation*, vol. 27, no. 9, pp. 1825–1856, 2015.
- [13] J. H. Macke, L. Buesing, J. P. Cunningham, M. Y. Byron, K. V. Shenoy, and M. Sahani, “Empirical models of spiking in neural populations,” in *Advances in Neural Information Processing Systems*, pp. 1350–1358, 2011.
- [14] M. M. Churchland, M. Y. Byron, J. P. Cunningham, L. P. Sugrue, M. R. Cohen, Corrado, *et al.*, “Stimulus onset quenches neural variability: a widespread cortical phenomenon,” *Nature Neuroscience*, vol. 13, no. 3, pp. 369–378, 2010.
- [15] J. F. Lawless, “Negative binomial and mixed poisson regression,” *Canadian Journal of Statistics*, vol. 15, no. 3, pp. 209–225, 1987.
- [16] Z. Chen, D. F. Putrino, S. Ghosh, R. Barbieri, and E. N. Brown, “Statistical inference for assessing functional connectivity of neuronal ensembles with sparse spiking data,” *IEEE Transactions on Neural Systems and Rehabilitation Engineering*, vol. 19, no. 2, pp. 121–135, 2011.
- [17] G. M. Cordeiro and P. McCullagh, “Bias correction in generalized linear models,” *Journal of the Royal Statistical Society. Series B (Methodological)*, pp. 629–643, 1991.

- [18] M. D. Mauk and D. V. Buonomano, “The neural basis of temporal processing,” *Annual Review of Neuroscience*, vol. 27, pp. 307–340, 2004.
- [19] N. Bertschinger and T. Natschläger, “Real-time computation at the edge of chaos in recurrent neural networks,” *Neural Computation*, vol. 16, no. 7, pp. 1413–1436, 2004.
- [20] J. Scott and J. W. Pillow, “Fully bayesian inference for neural models with negative-binomial spiking,” in *Advances in Neural Information Processing Systems*, pp. 1898–1906, 2012.
- [21] D. Goldfarb, “A family of variable-metric methods derived by variational means,” *Mathematics of Computation*, vol. 24, no. 109, pp. 23–26, 1970.
- [22] D. F. Shanno, “On broyden-fletcher-goldfarb-shanno method,” *Journal of Optimization Theory and Applications*, vol. 46, no. 1, pp. 87–94, 1985.
- [23] H. W. Kuhn, “Nonlinear programming: a historical view,” in *Traces and Emergence of Non-linear Programming*, pp. 393–414, Springer, 2014.
- [24] Y. Taniai and J. Nishii, “Optimality of upper-arm reaching trajectories based on the expected value of the metabolic energy cost,” *Neural Computation*, vol. 27, no. 8, pp. 1721–1737, 2015.
- [25] N. Gillis and F. Glineur, “Accelerated multiplicative updates and hierarchical ALS algorithms for nonnegative matrix factorization,” *Neural Computation*, vol. 24, no. 4, pp. 1085–1105, 2012.
- [26] J. L. Lefebvre, Y. Zhang, M. Meister, X. Wang, and J. R. Sanes, “ γ -protocadherins regulate neuronal survival but are dispensable for circuit formation in retina,” *Development*, vol. 135, no. 24, pp. 4141–4151, 2008.
- [27] S. W. Linderman and R. P. Adams, “Discovering latent network structure in point process data,” *arXiv preprint arXiv:1402.0914*, 2014.

Appendix

Table 3: The Summary of Variable Definitions

Variable	Definition
i	Time bin
j	Trial number at each time bin
y_{ij}	Spike count of j -th trial at i -th time bin
\boldsymbol{x}_i	Vector of regressors at i -th time bin
λ_i	Expectation of Poisson distribution
θ_i	$1 - \theta_i$ is the underlying firing rate
α_i, β_i	Parameters of Beta distribution
σ	Degree of freedom of prior distribution
$\boldsymbol{\omega}$	Vector of weights
$g(\cdot)$	Family of link functions
γ	Parameter determining specific form of link function
μ_i	Expectation of prior distribution
n_i	Number of trials at i -th time bin
\bar{y}_i	Mean spike count across all trials
π_i	Weight of the observation component of estimator at i -th time bin
K	Data length (the total number of bins)
A_i, B_{ij}, C_{ij}	Component of the gradients
p	Element number of $\boldsymbol{\omega}$
N	Total number of neurons
ζ	$(r, \boldsymbol{\omega}, \sigma, \gamma)$
\mathbf{k}	Vector of Lagrangian coefficients
m	Variable number from 1 to $N+3$
t	Iteration step
\mathbf{d}	Vector of search direction
Δ_t	Step length of iteration